HOLOGRAPHIC SUPERCONDUCTOR

Thesis

submitted in partial fulfillment of the requirements for the degree of

DOCTOR OF PHILOSOPHY

by

AHMED RIZWAN C.L

DEPARTMENT OF PHYSICS

NATIONAL INSTITUTE OF TECHNOLOGY KARNATAKA (NITK),

SURATHKAL, MANGALORE - 575 025

Octobar, 2018

DECLARATION

By the Ph.D Research Scholar

CERTIFICATE

ACKNOWLEDGEMENT

ABSTRACT

Contents

List of Figures

List of Tables

Chapter 1

Introduction

The word Physics means 'knowledge of nature'in Greek. Physics deals with understanding different phenomenons occurring in nature from subatomic particles to hypergiant stars. Behind these events, we can see four types of fundamental forces classified as *Weak, Strong, Electromagnetic and Gravitational*. In these, weak and strong forces act in nuclear size range responsible for decay processes and binding of nucleons,electromagnetic between charged particles and gravitational force acts universal on everything. Gravitational force is oldest one formulated in Isaac Newton's *Philosophiæ Naturalis Principia Mathematica*, decribes gravity as a universal force which attracts two bodies. Range and time scale of these forces is distinct, weak and strong interaction interact around femtometers, electromagnetic and gravitational forces interact over infinite range. Though four interactions are distinct in their properties, by seeing underlying symmetries there are lot of works done in casting these interactions as a unified one. In the late 18th century, studying the statistics behind black body spectrum lead to quantum mechanics which is based on the fact that in the microscopic world, we cannot determine position and momentum simultaneously and precisely ie, certain amount of uncertainty involved when we measure two conjugate quantities like position-momentum or energy-time. Again in the early 19th century, incompactability between laws of Galilean mechanics and electromagnetism lead to a new theory called special theory of relativity. By that time due to the work of Maxwell there was a strong notion that not the force,but field is fundamental in physics. On the other hand New-

tons law for gravitational to great extend was succes, lead to theoretical prediction of Neptune treating the discrepancies in orbits of Mercury and Uranus as a three-body problem. Three-body problem itself being challenging, beyond that was not possible. At the same time,the precession of perihelion of Mercury's orbit explained by Newtons theory showed deviation from actual rate. Again,Einstein's special theory postulates that no signal can travel faster than light thus prohibiting *Action at a distance*. Thus if the sun is removed in the solar system, earth will take at least 8 minutes to feel the effect. In reality, effect of the Sun is instantaneous and the Earth will change its orbit immediately. Insearch of a relativistic theory for gravity lead Einstein to formulate a geometrical theory for gravity called general theory of relativity in 1915.General relativity has been precise in understanding various phenomenona happening in the large distance scale. Starting from the perihelion precession of Mercury, gravitational red shift and graviational lensing Einstein's theory gave correct explanation to these astrophysical phenomena. The General theory of relativity is based on the principle of equivalence which states that one cannot distinguish the motion of freely falling body in a gravitational field and a uniformly accelerated frame in small enough regions of space-time. But now combining relativity with quantum mechanics hit many problems such as conservation of probability density, particle number conservation... This made people Feymann to think about quantum field theory, which originte from . A Grand Unified Theory (GUT) is a model in particle physics in which, at high energy, the three gauge interactions of the Standard Model that define the electromagnetic, weak, and strong interactions, or forces, are merged into a single force. Even though they appear at different energy scales they can be unified through a framework called Quantum field theory,at sufficient high energy. Electromagnetic force is familiar one encountered in daily life, acts between charged particles. Weak and strong being seen in nuclear decays and between nucleons, electromagnetic between charged particles and gravitational force acts universal on everything. From the newtons work, gravity is formulated as a force acts between two masses.

Black hole thermodynamics has become an important area of research in recent years due to its immense impact on understanding quantum gravity (Wald 2001), (Page

2005), (Hawking and Page 1983), (Bardeen et al. 1973), (Bekenstein 1972), (Bekenstein 1973), (Bekenstein 1974). This importance lies in the fact that the microscopic structure of the black hole is not well understood in the framework of quantum gravity. In this regard the study of black hole becomes inseparable topic since its theoretical domain includes quantum mechanics and general relativity. As a ray of hope in this cluttered scenario, classical thermodynamic study of asymptotically anti-de Sitter black hole emerged as the successor, equipped with critical phenomena and phase structure results backing the AdS/CFT correspondence (Maldacena 1999). This duality enabled us to treat the topics like quark gluon plasma and various systems in condensed matter physics with more confidence and new insights. Among all, a pathbreaking correspondence has been established by (Davies 1978),(Chamblin et al. 1999a), (Chamblin et al. 1999b) between the phase diagrams of charged AdS black hole and van der Waals fluids (Kubizňák and Mann 2012).

In the early stage of the developement of black hole thermodynamics the mass of a black hole has been identified with its energy. In another approach, the cosmological constant is treated as thermodynamic pressure with the aid of extended phase space and thus interpreting the mass of the black hole as chemical enthalpy rather than its energy (Kubizňák et al. 2017)(Dolan 2011). The study of black hole thermodynamics in the extended phase space enables us to identify new thermodynamic variable, volume of the black hole which is conjugate to pressure. These new identifications lead to the emergence of thermodynamic phase transitions with the condensed matter counterpart like van der Waals fluid which is of our interest in this paper. Thermodynamics of various AdS black holes showing similar thermodynamic behaviour lead to the conclusion that this phenomenon is a universal feature (Gunasekaran et al. 2012). Again classical thermodynamic concept of a heat engine is applied to black hole thermodynamics and a way to convert mechanical energy from the black hole is found (Johnson 2014).

1.0.1 Objectives

1.1 Organization of the Thesis

The thesis is organized as follows:

Chapter 2 presents a brief introduction of methodology is discussed.

In **Chapter 3**,

In **chapter 4**,

Chapter 5

In **chapter 6**,

Chapter 7 summarizes the findings of the present research work by highlighting the important results of the thesis along with conclusions.

Chapter 2

Thermodynamics in AdS black holes

2.1 Introduction

An interesting extension of black hole thermodynamics into the regime of Joule-Thomson (JT) expansion is carried out recently in the work of Ökcü and Aydıner Ökcü and Aydıner (2017). They have studied JT expansion of charged AdS black hole and later in Kerr AdS black hole (Ökcü and Aydıner 2018), wherein inversion curve and isenthalpic curves are studied and compared with the van der Waals fluid. As an extension this method is applied to a spacetime in d dimension (Mo et al. 2018). In another application the corrections of the quintessence on the Joule-Thomson (JT) effect of the Reissner Nordstrom anti de Sitter (RNAdS) black hole is reported (Ghaffarnejad et al. 2018). Recently, effects of Lovelock gravity and JT expansion in charged Gauss-Bonnet black hole has been studied (Mo and Li 2018) (Lan 2018).

The phase transitions in the evolution of the early Universe can give rise to topological defects like global monopole (Kibble 1976) (Vilenkin 1985). Historically the concept of magnetic monopole was first introduced by Dirac in 1931. Monopoles are formed from breaking of a gauge symmetry which carries a unit of magnetic flux (Vilenkin and Shellard 1994). The formation of monopoles can be compared with the elementary particle formation where SO(3) gauge symmetery is broken. In a seminal work, Barriola and Vilenkin (Barriola and Vilenkin 1989) obtained the black hole

metric with a global monopole which has a distinct topological structure compared to Schwarzschild black hole. The gravitational fields associated with global monopole lead to anisotropies in the microwave background radiation and this fluctuations created later evolve into galaxies and clusters. The Significance of the global monopole paramater in holographic superconductivity studied by Chen et al., showed that superconducting transition depends on the monopole parameter (Chen et al. 2010a). Recently the thermodynamics of this blackhole is studied by Deng et al., (Deng et al. 2018) , where it is reported that the presence of global monopole plays a vital role in van der Waals like phase transition.

This paper is organised as follows. In section 2.2 we discuss the details of the charged AdS black hole metric and its thermodynamic properties. This is followed by a section on (sect. 2.3) Joule Thomson expansion for van der Waals fluids where we briefly review the well known results in classical thermodynamics. In section 2.4 we explore JT expansion for charged AdS blackhole with global monopole. We derive expression for inversion temperature and study the nature of inversion curve and isenthalpic plots. We conclude that section by calculating the ratio between inversion temperature T_i and critical temperature T_c. The ratio is compared to the earlier calculations for Kerr-AdS black hole (Ökcü and Aydıner 2017) and charged AdS black hole(Ökcü and Aydıner 2018). In the last section we present our results.

2.2 The charged AdS black hole with global monopole

2.2.1 The Metric

In this section, we briefly review the thermodynamic properties of charged AdS black hole with global monopole. The simplest model that gives rise to the global monopole is described by the Lagrangian in which global S0(3) symmetry is broken to S0(2) spontaneously Barriola and Vilenkin (1989),

$$\mathcal{L}_{gm} = \frac{1}{2}\partial_\mu \Phi^a \partial^\mu \Phi^{*a} - \frac{\gamma}{4}\left(\Phi^a \Phi^{*a} - \eta_0^2\right)^2, \tag{2.1}$$

where Φ^a is a multiplet of scalar field, γ is a constant and η is the energy scale of symmetry breaking. The spherically-symmetric field configuration describing a monople is,

$$\Phi^a = \eta_0 h(r)\frac{x^a}{r} \tag{2.2}$$

where x^a is the cartesian coordinate and $x^a x^a = r^2$. We make the following metric ansatz,

$$d\tilde{s}^2 = -\tilde{f}(\tilde{r})d\tilde{t}^2 + \tilde{f}(\tilde{r})^{-1}d\tilde{r}^2 + \tilde{r}^2 d\Omega^2 \tag{2.3}$$

where $d\Omega^2 = d\theta^2 + \sin^2\theta d\phi^2$. The energy-momentum tensor is given by the equation,

$$T_{\mu\nu} = \frac{2}{\sqrt{-g}}\frac{\partial}{\partial g^{\mu\nu}}\left(\mathcal{L}_{gm}\sqrt{-g}\right) = 2\frac{\partial \mathcal{L}_{gm}}{\partial g^{\mu\nu}} - g_{\mu\nu}\mathcal{L}_{gm}.$$

Which gives,

$$T_{tt} = f(r)\left(\frac{\eta_0^2 h'^2 f(r)}{2} + \frac{\eta_0^2 h^2}{r^2} + \frac{1}{4}\gamma\eta_0^4(h^2-1)^2\right) \tag{2.4}$$

$$T_{rr} = \frac{1}{f(r)}\left(-\frac{\eta_0^2 h'^2 f(r)}{2} + \frac{\eta_0^2 h^2}{r^2} + \frac{1}{4}\gamma\eta_0^4(h^2-1)^2\right) \tag{2.5}$$

$$T_{\theta\theta} = r^2\left(\frac{\eta_0^2 h'^2 f(r)}{2} + \frac{1}{4}\gamma\eta_0^4(h^2-1)^2\right) \tag{2.6}$$

$$T_{\phi\phi} = r^2\sin^2\theta\left(\frac{\eta_0^2 h'^2 f(r)}{2} + \frac{1}{4}\gamma\eta_0^4(h^2-1)^2\right) \tag{2.7}$$

One can approximate $h(r) = 1$ outside the monopole core as $h(r)$ increases linearly for $r < (\eta_0\sqrt{\gamma})^{-1}$ and exponentialy tends to 1 when $r > (\eta_0\sqrt{\gamma})^{-1}$Barriola and Vilenkin (1989). Solving the Einstein equation gives,

$$\tilde{f}(\tilde{r}) = 1 - 8\pi\eta_0^2 - \frac{2\tilde{m}}{\tilde{r}}. \tag{2.8}$$

Now, in four dimensional AdS space the metric for a charged black hole with a global monopole can be written with,

$$\tilde{f}(\tilde{r}) = 1 - 8\pi\eta_0^2 - \frac{2\tilde{m}}{\tilde{r}} + \frac{\tilde{q}^2}{\tilde{r}^2} + \frac{\tilde{r}^2}{l^2}. \tag{2.9}$$

In the above equations $\tilde{m}$, $\tilde{q}$ and l are the mass parameter, electric charge parameter and AdS radius of the black hole, respectively. We make the following coordinate transformation,

$$\tilde{t} = (1-8\pi\eta_0^2)^{-1/2}t \ \ , \ \ \tilde{r} = (1-8\pi\eta_0^2)^{1/2}r \tag{2.10}$$

and introduce new parameters

$$m = (1-8\pi\eta_0^2)^{-3/2}\tilde{m} \ \ , \ \ q = (1-8\pi\eta_0^2)^{-1}\tilde{q} \ \ , \ \ \eta^2 = 8\pi\eta_0^2. \tag{2.11}$$

Finally we have the line element

$$ds^2 = -f(r)dt^2 + f(r)^{-1}dr^2 + (1-\eta^2)r^2d\Omega^2 \tag{2.12}$$

$$f(r) = 1 - \frac{2m}{r} + \frac{q^2}{r^2} + \frac{r^2}{l^2} \ \ , \ \ A = \frac{q}{r}dt. \tag{2.13}$$

In terms of the corresponding parameters the electric charge and ADM mass are given by

$$Q = (1-\eta^2)q \ \ , \ \ M = (1-\eta^2)m. \tag{2.14}$$

2.2.2 The Thermodynamics

The largest root of $f(r_+) = 0$ gives the black hole event horizon, where r_+ is the location of the event horizon of the black hole. One can use this to express the ADM mass as follows,

$$M = \frac{(1-\eta^2)}{2}r_+ + \frac{Q^2}{2r_+(1-\eta^2)} + \frac{r_+^3(1-\eta^2)}{2l^2}. \tag{2.15}$$

Note that the first law of thermodynamics and Smarr relation holds good for this black-hole, which reads as follows

$$dM = TdS + \Phi dQ + VdP \ \ , \ \ M = 2(TS - PV) + \Phi Q. \tag{2.16}$$

The entropy S of the blackhole is obtained from the area A_{bh} of the event horizon,

$$S = \frac{A_{bh}}{4} = \pi(1-\eta^2)r_+^2. \tag{2.17}$$

In the extended phase space the cosmological constant corresponds to the thermodynamic variable pressure and its conjugate quantity corresponds to the thermodynamic volume,

$$P = -\frac{\Lambda}{8\pi} = \frac{3}{8\pi l^2} \quad , \quad V = \frac{4}{3}\pi(1-\eta^2)r_+^3. \tag{2.18}$$

The Hawking temperature is obtained as follows

$$T = \left(\frac{\partial M}{\partial S}\right)_{P,Q} = \frac{1}{4\pi r_+}\left(1 + \frac{3r_+^2}{l^2} - \frac{Q^2}{(1-\eta^2)^2 r_+^2}\right). \tag{2.19}$$

It is clear from equations (2.15), (2.17), (2.18) and (2.19) that the thermodynamic variables of the black hole under investigation depends on η. Hence it is reasonable to suspect that the thermodynamic behavior of the black hole will rely on the symmetry breaking scale. As the slope of the $T-S$ graph is related to specific heat, it's posi-

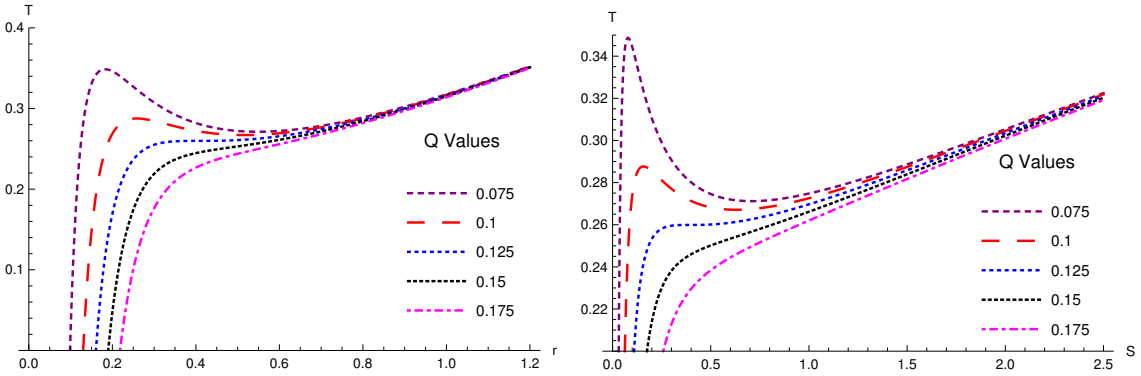

(a) (b)

Figure 2.1: Plots of T versus r_+ and T versus S for different values of Q and for $\eta = 0.5$. These plots shows the behavior of Hawking temperature.

tive and negative values are related to the stability and unstability of the system with respect to fluctuations. The plots 2.1(a) and **??** shows that there exists a critical point which indicates the phase transition. At this stage we recall from the literature that in a canonical ensemble where charge is fixed, the asymtotically AdS blackholes shows a first order phase transition similar to van der Waals fluids terminating in a second order

critical point.

2.2.3 Equation of state

Combining the expressions for Hawking temperature (eqn. 2.19) and the thermodynamic pressure (eqn. 2.18), we get the *equation of state* for a charged AdS blackhole with global monopole as,

$$P = \frac{T}{2r_+} - \frac{1}{8\pi r_+^2} + \frac{Q^2}{8\pi(1-\eta^2)^2 r_+^4}. \tag{2.20}$$

The above geometric equation of state is converted to physical equation of state under the dimensional analysis ground using the following scalings,

$$\tilde{P} = \frac{\hbar c}{l_P^2} P \ , \ \tilde{T} = \frac{\hbar c}{k} T, \tag{2.21}$$

where l_P is the Planck length. Comparing geometric equation of state with van der Waals equation, one can relate the specific volume v with the horizon radius r_+ as $v = 2l_P^2 r_+$. Using these relations the physical equation of state is obtained to be

$$P = \frac{T}{v} - \frac{1}{2\pi v^2} + \frac{2Q^2}{\pi(1-\eta^2)^2 v^4}. \tag{2.22}$$

At the critical point,

$$\left(\frac{\partial P}{\partial v}\right)_T = \left(\frac{\partial^2 P}{\partial v^2}\right)_T = 0. \tag{2.23}$$

Using this, the critical quantities are obtained as

$$P_c = \frac{(1-\eta^2)^2}{96\pi Q^2} \ , \ v_c = \frac{2\sqrt{6}Q}{1-\eta^2} \ , \ T_c = \frac{1-\eta^2}{3\sqrt{6}\pi Q^2}. \tag{2.24}$$

From these formulas, it is clear that the presence of global monopole term affects the critical pressure P_c, critical temperature T_c and the critical volume v_c compared to the Reissner-Nordström AdS black hole; P_c and T_c decreases while v_c increases.

2.3 Joule Thomson expansion

2.3.1 Joule-Thomson effect

Joule-Thomson effect is an irreversible adiabatic expansion of a gas when the gas is pushed through a porous plug. In this process, a non-ideal gas undergoes continuous throttling process which leads to a temperature change in the final state. When the gas in the higher pressure side having pressure P_i and temperature T_i is made to expand through a porous plug, the gas passes through dissipative non-equilibrium states due to the friction between the gas and the plug. Usual thermodynamic coordinates cannot be used to define these non-equilibrium states, but it is found that enthalpy which is the sum of internal energy and product of pressure volume remains same in the final state (Zemansky et al. 2011). So a state function called *enthalpy* $H = U + PV$ is defined, which remains unchanged in the end states,

$$H_i = H_f \tag{2.25}$$

It is not entitled to say that enthalpy is a constant during this process, since enthalpy is not defined when gas traverses non-equilibrium states. The set of discrete points in the phase diagram initial point (P_i, T_i) and all other points P_fs and T_fs representing equilibrium states of some gas having same molar enthalpy (h) at initial and all the final equilibrium states. These discrete points corresponding to same molar enthalpy lies on a smooth curve known as *isenthalpic curve*. To summarise an isenthalpic curve is the locus of all points with the same molar enthalpy representing intial and final equilibrium states. A set of such curves can be obtained for different values of enthalpy.

The slope of an isenthlpic curve on $T - P$ plane is called the *Joule Thomson coefficient* μ_J.

$$\mu_J = \left(\frac{\partial T}{\partial P}\right)_H. \tag{2.26}$$

Joule Thomson coefficient is zero at the maxima of the isenthalpic curve. The locus of such points is called inversion curve. The interior of the inversion curve where the gradient of isenthalps (μ_J) positive is called region of cooling and the exterior where μ_J

is negative called the region of heating. The differential of molar enthalpy is given by

$$dh = Tds + vdP. \tag{2.27}$$

We recall the second TdS equation in classical thermodynamics (Zemansky et al. 2011)

$$TdS = C_P dT - T\left(\frac{\partial v}{\partial T}\right)_P dP. \tag{2.28}$$

Using equation(2.28) in equation(2.27),

$$dT = \frac{1}{C_P}\left[T\left(\frac{\partial v}{\partial T}\right)_P - v\right]dP + \frac{1}{C_P}dh. \tag{2.29}$$

Which gives

$$\mu_J = \left(\frac{\partial T}{\partial P}\right)_H = \frac{1}{C_P}\left[T\left(\frac{\partial v}{\partial T}\right)_P - v\right]. \tag{2.30}$$

As $\mu_J = 0$ defines the inversion temperature we have

$$T_i = V\left(\frac{\partial T}{\partial v}\right)_P. \tag{2.31}$$

2.3.2 van der Waals fluid

van der Waals gas is the simplest model used to explain the behaviour of the real gases, which departs from the ideal gas discription with richer outcomes as it includes the intermolecular interaction and the non zero size of the molecules. The equation of state for a van der Waals gas is given by,

$$\left(P + \frac{a}{V_m^2}\right)(V_m - b) = RT. \tag{2.32}$$

Here the constants a and b parameterizes the strength of the intermolecular interaction and the volume excluded due to the finite size of the molecule, respectively. The equation of state reduces to ideal gas equation under the limit a and b both set to zero. We used V_m for molar volume, which is simply V for one mole of substance.

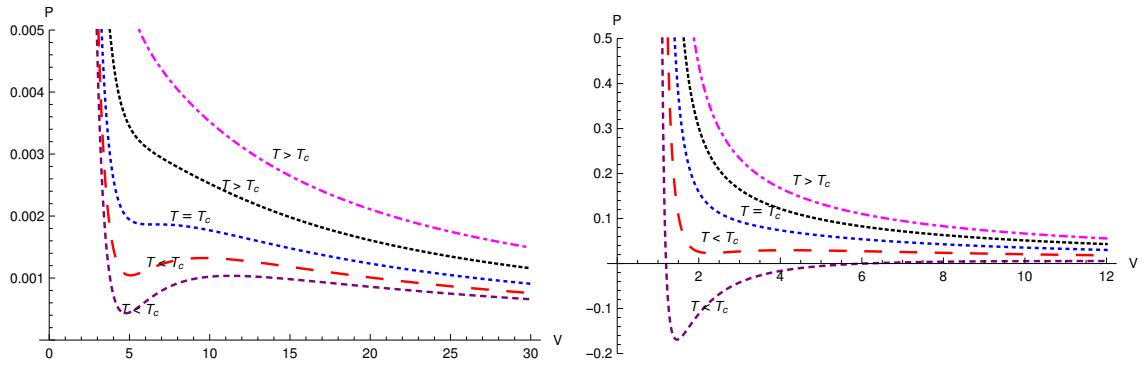

(a) (b)

Figure 2.2: Fig 2.2(a) is isotherms of the van der Waals gas with temperature decreases from top to bottom. Fig 2.2(b) shows $P-v$ diagram of charged AdS blackhole with global monopole where the parameters are choosen to be $Q=1$ and $\eta=0.5$. Similar $P-v$ diagrams can be obtained for different values of η. Variation of η does not changes the nature of the $P-v$ diagram even though it changes the critical parameters.

To calculate the critical points namely the temperture T_c, pressure P_c and volume V_c we rearrange the equation of state (equation 2.32) for P as follows,

$$P=\frac{RT}{V-b}-\frac{a}{V^2}. \tag{2.33}$$

Using this equation the $P-v$ isotherms are plotted for van der Waals gas in fig. 2.2(a). Fig 2.2(b) is the $P-v$ diagram of the charged AdS black hole, which is obtained from equation (2.22), is having a typical behavior of a van der Waals fluid. In both these graphs below a certain point called critical point there are inflection points and above that a monotonic behavior is displayed. This is a general result for AdS black holes (Kubizňák and Mann 2012). At the critical point $\left(\frac{\partial P}{\partial V}\right)_T=\left(\frac{\partial^2 P}{\partial V^2}\right)_T=0$, which gives

$$V_c=3b \quad , \quad T_c=\frac{8a}{27Rb} \quad P_c=\frac{a}{27b^2}. \tag{2.34}$$

The internal energy of van der Waals gas is given by (Landau et al. 1980)

$$U(T,v)=\frac{3}{2}k_BT-\frac{a}{v}. \tag{2.35}$$

Making a Legendre transformation $H = U + PV$ we obtain the expression for enthalpy,

$$H(T,v) = \frac{3}{2}k_BT + \frac{k_BTv}{v-b} - \frac{2a}{v}. \tag{2.36}$$

The inversion temperature is calculated from equation (2.31)

$$T_i = \frac{1}{k_B}\left(P_iv - \frac{a}{v} + \frac{2ab}{v^2}\right) \tag{2.37}$$

and from equation of state (equation 2.32) we have

$$T_i = \frac{1}{k_B}\left(P_iv - P_ib + \frac{a}{v} - \frac{ab}{v^2}\right). \tag{2.38}$$

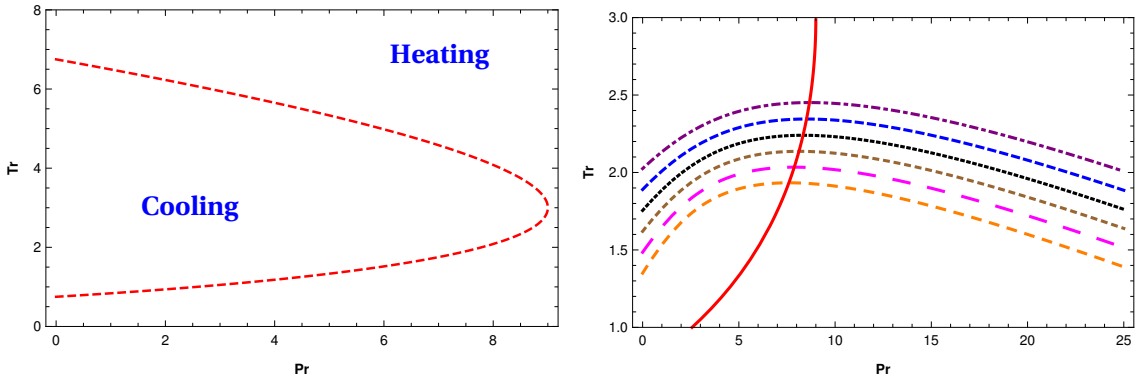

(a) (b)

Figure 2.3: In fig. 2.3(a) inversion curve separating the regions of heating and cooling are shown. In fig 2.3(b) isenthalpic curves for different values of enthaly is plotted along with the lower half of inversion curve for the van der Waals gas. While ploting this, we worked with dimensionless coordinates i.e., reduced pressure $P_r = P/P_c$ and reduced temperature $T_r = T/T_c$.

Equations (2.37) and (2.38) gives

$$Pbv^2 - 2av + 3ab = 0. \tag{2.39}$$

Solving the above equation for v and substituting in equation of state (equation 2.32)

we obtain

$$T_i = \frac{2\left(5a - 3b^2P_i \pm 4\sqrt{a^2 - 3ab^2P_i}\right)}{9bk_B}. \tag{2.40}$$

Using this we plot the inversion curves fig. 2.3(a). In fig. 2.3(b) isenthalpic and inversion curves are shown together. For the sake of comparison later with the isenthalpic-inversion curve of black hole we have taken only lower half of T_i.

2.4 Joule Thomson expansion of charged AdS black-hole with monopole term

In this section we study the JT expansion of charged AdS black hole with monopole term. Because of the treatment of black hole mass equivalent to enthalpy in extended phase space the isenthalpic plots are replaced by constant mass plots in this case (for brevity we still call it as isenthalpic curve).

Recall the expression for Joule Thomson coefficient

$$\mu_J = \left(\frac{\partial T}{\partial P}\right)_M = \frac{1}{C_P}\left[T\left(\frac{\partial V}{\partial T}\right)_P - V\right]. \tag{2.41}$$

From this we obtain the the invesion temperature

$$T_i = V\left(\frac{\partial T}{\partial V}\right)_P. \tag{2.42}$$

For this we rewrite the equation of state interms of V as follows

$$\begin{aligned} T = &\left(\frac{(1-\eta^2)}{48\pi^2}\right)^{1/3}\frac{1}{V^{1/3}} + P\left(\frac{6}{\pi(1-\eta^2)}\right)^{1/3}V^{1/3} \\ &- \frac{Q^2}{3(1-\eta^2)}\frac{1}{V}. \end{aligned} \tag{2.43}$$

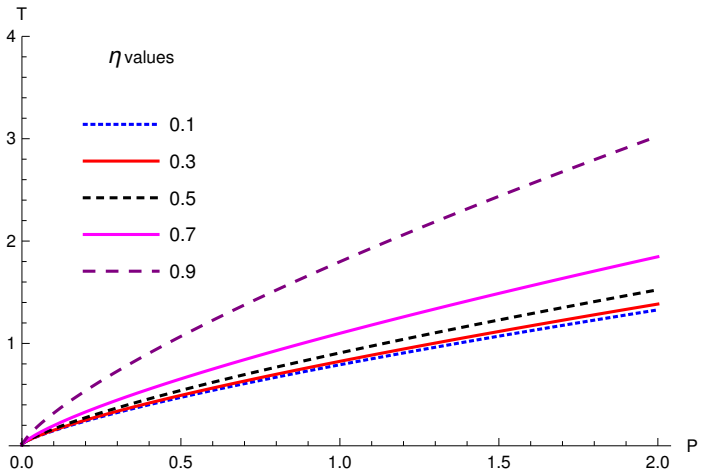

Figure 2.4: Effect of monopole term η on inversion curve. Here we have chosen different values of monopole ($\eta = 0$ to 0.9 in steps) by keeping charge Q fixed.

Substituting this into equation (2.42) we have the inversion temperature

$$T_i = -\frac{1}{6}\left(\frac{(1-\eta^2)}{6\pi^2}\right)^{1/3}\frac{1}{V^{1/3}} + P\left(\frac{2}{9\pi(1-\eta^2)}\right)^{1/3}V^{1/3} + \frac{Q^2}{3(1-\eta^2)}\frac{1}{V} \tag{2.44}$$

$$= \frac{Q^2}{4\pi r_+^3(1-\eta^2)^2} + \frac{2}{3}Pr_+ - \frac{1}{12\pi r_+}. \tag{2.45}$$

From equation(2.20) we have

$$T_i = -\frac{Q^2}{4\pi r_+^3(1-\eta^2)^2} + 2Pr_+ + \frac{1}{4\pi r_+}. \tag{2.46}$$

From equation (2.45) and equation (2.46) we get

$$8\pi(1-\eta^2)^2Pr_+^4 + 2(1-\eta^2)^2r_+^2 - 3Q^2 = 0. \tag{2.47}$$

Solving the above for r_+ and choosing the following appropriate root (actually we get four roots for equation (2.47), the other three are complex),

$$r_+ = \frac{1}{2\sqrt{2\pi}}\sqrt{\frac{\sqrt{\left((1-\eta^2)^2 + 24\pi PQ^2\right)}}{(1-\eta^2)P} - \frac{1}{P}}. \tag{2.48}$$

Substituting this root into equation (2.46)

$$T_i = \frac{\sqrt{P_i}\left(1+\frac{16\pi P_i Q^2}{(1-\eta^2)^2}-\frac{\sqrt{24P_i\pi Q^2+(1-\eta^2)^2}}{(1-\eta^2)}\right)}{\sqrt{2\pi}\left(-1+\frac{\sqrt{24P_i\pi Q^2+(1-\eta^2)^2}}{(1-\eta^2)}\right)^{3/2}}. \tag{2.49}$$

From this equation the inversion curves are plotted for different values of η (fig 2.5). From the graphs one can infer that the JT coefficient μ_J is sensitive to η values i.e., μ_J increases with η. In fig. (2.4), this inference is depicted taking different η values in the same plot for a fixed Q value.

By demanding $P_i = 0$, we obtain T_i^{min}

$$T_i^{min} = \frac{(1-\eta^2)}{6\sqrt{6}\pi Q}. \tag{2.50}$$

Using this we calculate the ratio between T_i^{min} and T_c as

$$\frac{T_i^{min}}{T_c} = \frac{1}{2}. \tag{2.51}$$

This is an interesting result which matches with the earlier established resultS for the charged AdS blackhole (Ökcü and Aydıner 2017), Ökcü and Aydıner (2018). At the end of this study, we plot isenthalpic curves for various combinations of η and Q in the $T-P$ plane. Inverse points (T_i, P_i) on $T-P$ plane seperates heating phase from the cooling phase of JT expansion. Recall that isenthalpic curve in this case is not a plot with constant enthalpy, rather constant mass. The crossing diagram between inversion and isenthalpic curve shown in fig. (2.6) displays the sensitivity of inverse points (T_i, P_i) for the different values of η and Q. All our calculations and graphs shows that when global monopole parameter is zero, the results nicely reduces to the earlier studies on JT expansion of charged AdS black holes.

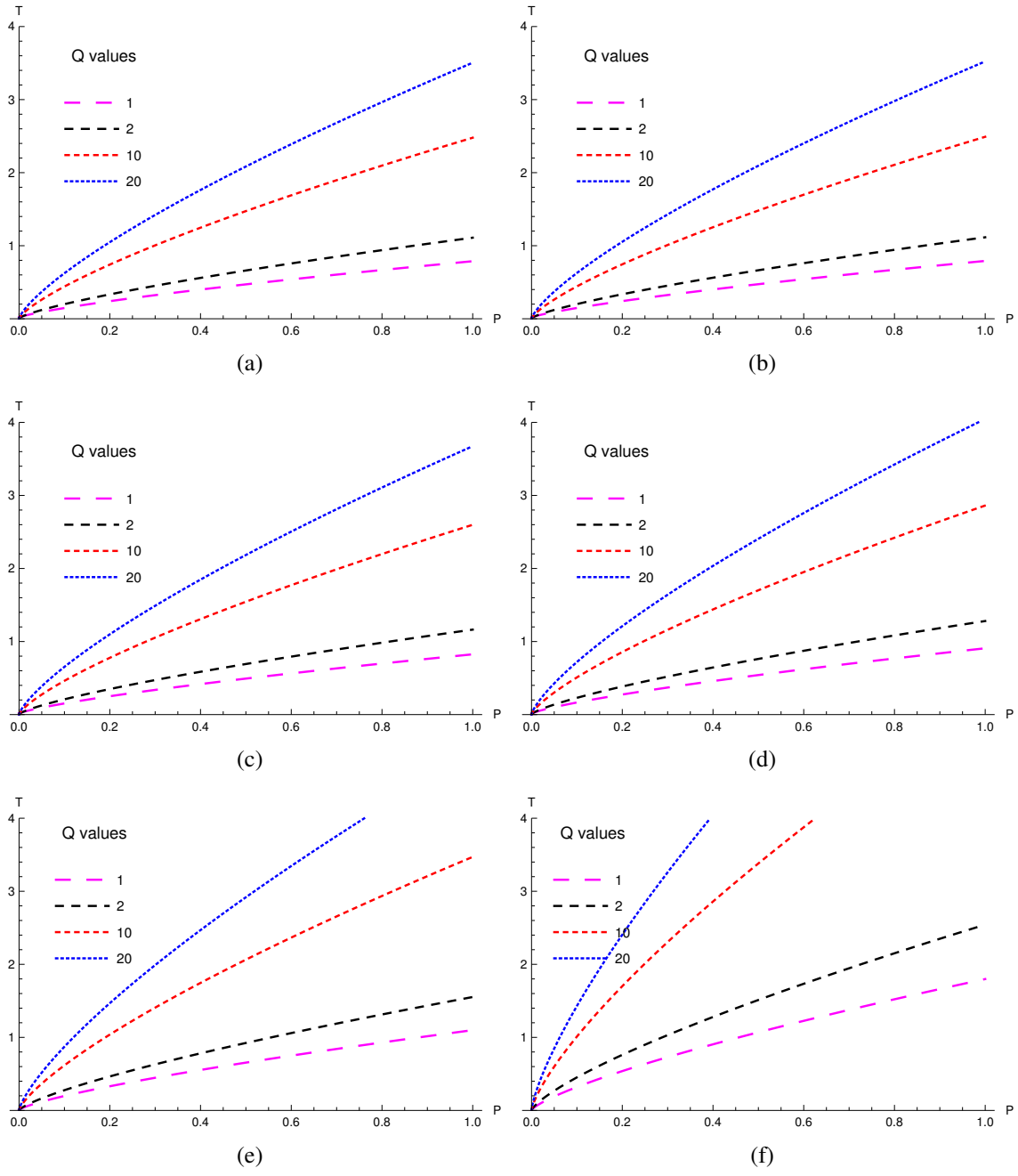

Figure 2.5: Inversion curves for charged AdS black hole with global monopole parameter $\eta = 0, 0.1, 0.3, 0.5, 0.7, 0.9$ from top to bottom. The plots are the locus of inversion ponts (P_i, T_i). Increasing η increases the inversion temperature for fixed pressure.

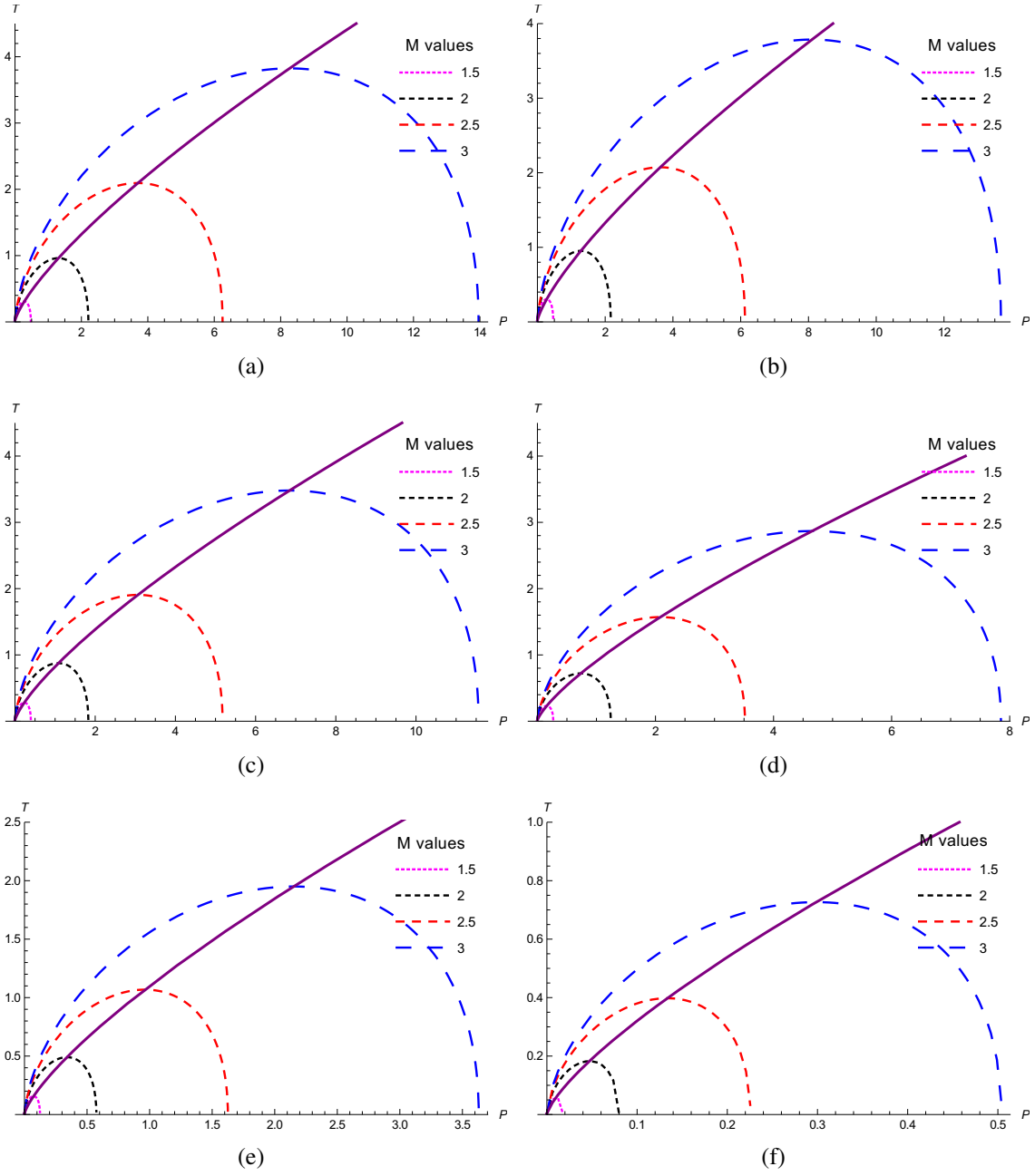

Figure 2.6: Crossing diagrams between inversion and isenthalpic curves for different values of η. ($\eta = 0, 0.1, 0.3, 0.5, 0.7, 0.9$ from top to bottom and $Q = 1$).

2.5 Conclusions

In this paper, we have explored the Joule Thomson expansion for AdS black hole with global monopole in extended phase space. Firstly, we studied the thermodynamic properties of the black hole and analysed the effect of η on these properties. Then the JT coefficient μ which determines the cooling and heating phase was obtained for van der Waals gas. This is followed by the observation of inversion and isenthalphic curves for the same gas.

We applied the idea of JT expansion to charged AdS black hole with global monopole whereby our key ingredient was the symmetry breaking parameter η. The tradtional JT coefficient analysis, isenthalpic and inversion curve studies were done for this metric with different values of η. The result is interesting one where we have noticed that the dependence of thermodynamic behaviour on η is crucial. The inversion temperature and pressure both increases monotonically with η, which is evident from the inversion and isenthalpic curves. From the inversion curves we conclude that the sensitivity of T_i for a given value of P_i with increasing η is stringent.

It is a well known fact that the topological deffects plays an interesting role in galaxy formation and baryogenesis in several theoretical approaches. Hence we hope that the study of JT expansion with monopole term will be significant from different perspectives. As an extension of this work in future, we seek the significance of cooling and heating in JT expansion related to super cooling phase in cosmological transitions.

Chapter 3

Holographic superconductivity in AdS black holes

3.1 Introduction

The gauge/gravity duality or AdS-CFT correspondence is a novel approach to solve strongly correlated systems. The AdS-CFT correspondence opened a new window connecting strongly coupled condensed matter physics with its dual classical gravity system **?**. Understanding strongly coupled systems such as high-Tc superconductivity in cuprates and quantum chromodynamics at low energy scales becomes tractable via this duality. In 2008, using an Abelian-Higgs model, Gubser showed that a black hole in Anti-deSitter spacetime is unstable with respect to the development of scalar hair. When cooled below a certain Hawking temperature U(1) symmetry of the Higgs fields is spontaneously broken **?**. The complex scalar field gains a non-zero vacuum expectation value and a charged condensate forms near the event horizon. Sean Hartnoll showed that the AdS/CFT correspondence could be used to connect the formation of a charged condensate at the black hole horizon with the onset of superconductivity in the conformal field theory living on the boundary of the AdS spacetime. According to AdS-CFT dictionary, the current operator J^{μ} and the stress- energy tensor $T^{\mu\nu}$ on the boundary are dual to the gauge field A_{μ} and the metric $g_{\mu\nu}$ in the bulk. And the complex scalar field ψ in the bulk will have dual operator $\mathcal{O}$ in the boundary which gives

the condensate. The charged scalar field develos a non-zero vaccum expectation value during the spontaneous symmetry breaking of U(1) field. Initialy, holographic model was develped for s-wave high temperature superconductors, later extended to p and d-wave superconductors. The p-wave superconductors were constructed using SU(2) Yang-Mills field as gauge theory which develops a vector hair below T_c and d-wave model by considering spin-two field coupled to U(1) field.

In this paper, we study properties of holographic superconductors formed in Garfinkle-Horowitz-Strominger (GHS) dilaton black hole. GHS black hole is the stringy analog of Reissner-Normstom black holes in general relativity**?**. We study the superconductivity in the magnetically charged GHS black holes and the themodynamic geometry of this black hole, which shows a second order phase transition near horizon.

3.1.1 Magnetically charged GHS black holes

Though black holes predicted in string theory is different from classical solutions, when the mass parameter is comparable with the Planck mass static uncharged black hole in string theory is approximated as Schwarzschild solution. But it is not true for charged black holes, the spherically symmetric static charged black hole solution in low energy heterotic string theory was pointed out by Gibbons, Maeda, Garfinkle, Horowitz and Strominger . The action for magnetically charged low energy heterotic string theory can be written in general form as,

$$S = \int d^D x \sqrt{-g} e^{-2\phi} [\Lambda + R + 4(\nabla\phi)^2 - F^{\mu\nu}F_{\mu\nu} - \frac{1}{12} H_{\mu\nu\rho} H^{\mu\nu\rho}]$$

where ϕ is dialaton field, $F^{\mu\nu}$ a Maxwell's field and $H_{\mu\nu\rho}$ is a 3-form $H = dB - F \wedge F$ and $dH = -F \wedge F$. We restrict form field H and cosmological constant Λ to zero. The metric for the magneticaly charged black hole in Einstein-frame is given by,

$$ds^2 = -\frac{f(r)}{a(r)} dt^2 + \frac{dr^2}{f(r)a(r)} + r^2 d\theta^2 + r^2 \sin^2\theta d\phi^2$$

where $f(r) = 1 - \frac{2M}{r}$ and $a(r) = 1 - \frac{Q^2}{Mr}$. M and Q are the mass and magnetic charge of black hole **??**.

The Hawking temperature of this black hole is same as for Schwarzchild case, because in the r-t plane metric is identical. The GHS black hole can be embeded in AdS space as,

$$ds^2 = -\frac{1-\frac{2M}{r}+\frac{r^2}{L^2}}{1-\frac{Q^2}{Mr}}dt^2 + \frac{dr^2}{\left(1-\frac{2M}{r}+\frac{r^2}{L^2}\right)\left(1-\frac{Q^2}{Mr}\right)} + r^2 d\theta^2 + r^2\sin^2\theta d\phi^2 \tag{3.1}$$

where L is the AdS radius.

3.2 Holographic superconductors

Minimum ingredient required for holographic superconductor contains Maxwell's field and a charged complex scalar field in a charged black hole background**?**. The holographic action is given by,

$$S = \int d^4x\sqrt{-g}\left(R + \frac{6}{L^2} - \frac{1}{4}F_{\mu\nu}F^{\mu\nu} - g^{\mu\nu}(D_\mu\psi)^*(D_\nu\psi) - m^2|\psi|^2\right) \tag{3.2}$$

where R is the Ricci scalar, $\frac{6}{L^2}$ is the AdS term with negative curvature or cosmological constant. Here gravitational field is coupled to a Maxwell's field and complex scalar field with mass m and charge q. Equation of motion for scalar field ψ and Maxwells field A_μ is given by,

$$\frac{1}{\sqrt{-g}}\partial_\mu\left(\sqrt{-g}g^{\mu\nu}\left(\partial_\nu\psi - iA_\nu\psi\right)\right) - ig^{\mu\nu}A_\mu\left(\partial_\nu\psi - iA_\nu\psi\right) + \frac{2}{L^2}\psi = 0 \tag{3.3}$$

$$\frac{1}{\sqrt{-g}}\partial_\nu\left(\sqrt{-g}g^{\nu\lambda}g^{\mu\sigma}F_{\lambda\sigma}\right) - g^{\mu\nu}\left(i\left(\bar{\psi}\partial_\nu\psi - \partial_\nu\bar{\psi}\psi\right) + 2A_\nu\bar{\psi}\psi\right) = 0 \tag{3.4}$$

Taking ansatz for fields as $\psi = \psi(r)$ and $A_\mu = (\phi, 0, 0, 0)$, evaluating scalar equation 3.3 and Maxwell's equation 3.4 in the metric ansatz 3.1, we obtain ,

$$\psi'' + \left(\frac{f'(r)}{f(r)} + \frac{2}{r}\right)\psi' + \left(\frac{2}{f(r)L^2} - \frac{1}{f(r)^2}\phi^2\right)\psi = 0 \tag{3.5}$$

$$\phi'' + \left(\frac{2}{r} + a'(r)\right)\phi' - \frac{2\psi^2}{f(r)}\phi = 0 \tag{3.6}$$

The Hawking temperature can be found as,

$$T_H = \frac{3}{4\pi} r_+ \tag{3.7}$$

where r_+ is the horizon radius. The asymptotic value of the scalar field ψ and the scalar potential ϕ near the boundary $(r \to \infty)$ are,

$$\psi = \frac{\psi^{(1)}}{r} + \frac{\psi^{(2)}}{r^2} + \cdots$$
$$\phi = \mu - \frac{\rho}{r} + \cdots .$$

where μ is the chemical potential and ρ is the charge density of the conformal field theory. Change of coordinate $z = \frac{r_+}{r}$, so that the horizon is located at z=1 and the boundary is at z=0. Equations 3.5 3.6 reduces to,

$$z^2\psi''(z) + \frac{z^2 f'(z)}{f(z)}\psi'(z) + \left(\frac{2 + z f'(z)}{f(z)} + \frac{z^2\phi^2(z)}{f^2(z)} - 2\right)\psi(z) = 0 \tag{3.8}$$

$$\phi''(z) - \frac{a'(z)}{z^2}\phi'(z) - \frac{2\psi^2(z)}{f(z)}\phi(z) = 0 \tag{3.9}$$

We solve these two coupled ordinary differential using shooting method. First Taylor series expansion of the fields around the horizon z= 1 and boundary z=0,

$$\begin{aligned}
\psi_h(z) =& a(z-1) + b(z-1)^2 + c(z-1)^3 + d(z-1)^4 .\\
\phi_h(z) =& A + B(z-1) + C(z-1)^2 + D(z-1)^3 + D(z-1)^4\\
\psi_b(z) =& a_1 + b_1 z + c_1 z^2 + d_1 z^3 .\\
\phi_b(z) =& A_1 + B_1 z + C_1 z^2 + D_1 z^3 .
\end{aligned}$$

Solving for the coefficients a_1, b_1, A_1 and B_1 which corresponds to $\psi^{(1)}$, $\psi^{(2)}$, μ and ρ respectively.

From the AdS/CFT dictionary, scalar field ψ sources a scalar operator $\mathcal{O}$ in the field theory. Turning off one of the sources $\psi^{(1)}$ or $\psi^{(2)}$ leads to spontaneous breaking of $U(1)$ field and the scalar operator $\mathcal{O}$ develops a non-trivial vacuum expectation value. The expectation-value of the scalar operators $\mathcal{O}_1$ and $\mathcal{O}_2$ on the boundary dual to the

fields in the bulk is read as,

$$\langle \mathcal{O}_1 \rangle = \sqrt{2}\psi^{(1)}, \qquad \langle \mathcal{O}_2 \rangle = \sqrt{2}\psi^{(2)} \tag{3.10}$$

To make the quantities scale invariant, we define

$$\langle \mathcal{O}_1 \rangle = \frac{\langle \mathcal{O}_1 \rangle}{\sqrt{\rho}}, \qquad \langle \mathcal{O}_2 \rangle = \frac{\langle \mathcal{O}_2 \rangle}{\rho} \tag{3.11}$$

The expectation values of operators $\mathcal{O}_1$ and

$\mathcal{O}_2$ is plotted against temperature T varyingFigure shows that the charged bosonic magnetic charge Q.
condensate $\langle \mathcal{O} \rangle$ is formed below T_c , matching with predictions of Landau-Ginzburg theory for a second order phase transition.

3.3 Optical Conductivity

The optical conductivity also can be computed in dual CFT by fluatuating electromagnetic field in the bulk, which gives the conductivity in the boundary,

$$A_x'' + \frac{f'}{f}A_x' + \left(\frac{\omega^2}{f^2} - \frac{2\psi^2}{f}\right)A_x = 0 \tag{3.12}$$

From AdS-CFT dictionary,

$$\sigma(\omega) = \frac{1}{i\omega}G^R(\omega) = \frac{1}{i\omega}\frac{A^{(1)}}{A^{(0)}}$$

At temperatures below T_c the optical conductivity develops gap at a gap frequency ω_g. We find here the gap frequency $\omega_g = 8T_c$, which islarge compared to BCS case $\omega_g = 3.5T_c$, indicating strong coupling in fermionic pairs. This holographic model exhibits the properties of superconductors such as formation of charged condensate below T_c through a second order phase transition, infinite DC conductivity and gaped optical conductivity at small frequencies.

3.4 Results and discussions

Chapter 4

Thermodynamic geometry in AdS black holes

4.1 Introduction

In recent years, black hole thermodynamics has become an active area of research in theoretical physics. Among several motivations, the main attraction lies in the fact that, black hole is the best system to seek the aspects of quantum gravity, and the thermodynamic study will reveal its microscopic structure. Introduction of a correspondence between classical gravitational theory in AdS space and strongly coupled conformal field theory on its boundary by Maldacena in his seminal paper (Maldacena 1999) made the thermodynamic study of asymptoticaly AdS black holes more interesting. The black hole thermodynamics in anti-de Sitter (AdS) space is different from asymptotically Minkowskian spacetime. The AdS space acts like a thermal cavity and black hole can exist in a stable equilibrium with radiation. But there is a minimum Hawking temperature (critical temperature) below which only thermal radiation exists. Above this temperature two types of black hole solutions exists, a smaller black hole with negative specific heat capacity and a larger black hole with positive specific heat capacity. At critical temperature, Hawking-Page phase transition takes place between thermal radiation and large black hole (Hawking and Page 1983). In the AdS-CFT perspective, Hawking-Page phase transition is understood as confinement/deconfinement

phase transition in gauge theory (**?**).

Realising the importance of the thermodynamics in AdS space, the Reissner-Nordström and the Kerr-Newman black holes in AdS background were studied. The small-large black hole phase transition found in RN-AdS had a close resemblence to van der Waals liquid-gas system (Chamblin et al. 1999a, **?**, **?**). More clarity on this isomorphism was obtained by identifying the cosmological constant as thermodynamic pressure and by expanding first law by including a PdV term (**????**). Recently, thermodynamics of various black holes in this extended phase space were studied and the similarity with van der Waals liquid-gas system was found to be universal (**???????**).

After Albert Einstein's theory of gravity based on differential geometry became a great success, method of differential geometry was identified as a mathematical language for various gauge fields. It was Gibbs (**?**) in the later part of 19th century and Caratheodory (**?**) in 1909, to use these ideas of differential geometry in classical thermodynamics. Hermann (**?**) and Mrugala (**?**), applied differential geometry to the thermodynamic phase space making use of its contact structure. Then Weinhold (**?**) and later Ruppeiner (**??**) constructed thermodynamic metric to study phase transitions and microscopic interactions in thermodynamic systems. Geometrothermodynamics is another geometric formalism for the classical thermodynamics developed by H.Quevedo (**?**). Recently, a brief history of metric geometry of thermodynamics was written by Ruppeiner (**?**). From these geometric formalisms, a metric is defined on equilibrium thermodynamic state space and the thermodynamic curvature scalar encodes the information about the microscopic interactions. The curvature scalar is propotional to the correlation volume and its sign tells the nature of microscopic interactions being attractive or repulsive (**?**). The phase transition of the system can be seen in the divergence behavior of this curvature scalar near the critical point. Thermodynamic geometry is applied to van der Waals gas and different statistical models including magnetic models (**??????**).

Considering black hole as a thermodynamic system, the geometric formalism is used to study the critical behavior of black holes during phase transitions (**??????**Sahay et al. 2010, **?**, **?**, **?**, **?**, **?**, **?**, **?**, **?**, **?**, **?**, **?**, **?**, **?**, **?**, **?**, **?**, **?**, **?**, **?**). But there were inconsistencies

in the position of critical point, as specific heat diverges at a point different from where scalar curvature diverges (**???**). The Legendre invariance was found to be the key factor behind these discrepancies. Taking Legendre invariance into account a metric was constructed by Quevedo et al. (**???**), which resolved the issue. Quevedo's formalism named as Geometrothermodynamics(GTD) is applied to various black holes (**???????**) including regular black holes. A black hole without singularity at the origin, possessing an event horizon is called regular or non-singular black hole. It was Bardeen (**?**) in 1968, who constructed a black hole solution with regular non-singular geometry with an event horizon for the first time. Later, several such regular black hole solutions were constructed (**??**). Thermodynamic properties of Bardeen regular black hole was studied in (**?**).

Accelerated expansion of universe is due to presence of exotic field called Dark energy. Quintessence is one among different models for dark energy (**???**). The cosmic source for inflation has the equation of state $p_q = \omega\rho_q$ ($-1 < \omega < -1/3$), and $\omega = -2/3$ corresponds to quintessence dark energy regime. The energy density for quintessence has the form $\rho_q = -\frac{a}{2}\frac{3\omega}{r^{3(\omega+1)}}$, which is positive for usual quintessence. Several attempts have been made to explore the effects of quintessence on black hole, with Kiselev's (**?**) phenomelogical approach being the notable one. Phase transitions in black holes surrounded by quintessence are widely studied. Thermodynamics of Reissner-Nordström and regular black holes surrounded by quintessence were investigated in (**???????**). Thermodynamic geometry and geometrothermodynanics for different regular black holes were studied in (**?**). Thermodynamic geometry of charged AdS black hole surrounded by quintessence can be found in (**?**).

This paper is organised as follows. In section 4.2, thermodynamics of regular Bardeen black hole surrounded by quintessence is studied in the extended phase space. In the next section (4.3), thermodynamic geometry for the black hole is constructed using Weinhold and Ruppeiner metric, followed by geometrothermodynamics. Conclusion is written in the final section (4.4).

4.2 Thermodynamics of the black hole

The metric for the regular Bardeen AdS black hole surrounded by quintessence is given by (**????**),

$$ds^2 = -f(r)dt^2 + \frac{dr^2}{f(r)} + r^2 d\theta^2 + r^2 \sin^2\theta d\phi^2$$

with $f(r) = 1 - \frac{2\mathcal{M}(r)}{r} - \frac{a}{r^{3\omega+1}} - \frac{\Lambda r^2}{3}$ and $\mathcal{M}(r) = \frac{Mr^3}{(r^2+\beta^2)^{3/2}}$. Where β is the monopole charge of a self gravitating magnetic field described by non linear electromagnetic source, M is the mass of the black hole, Λ is the cosmological constant, ω is the state parameter and a is the normalization constant related to quintessence density.

On the event horizon (r_h) , $f(r_h) = 0$ gives the mass corresponding to the above metric,

$$M = \frac{1}{6} r_h^{-3(1+\omega)} (\beta^2 + r_h^2)^{3/2} [-3a + r_h^{1+3\omega}(3 + 8P\pi r_h^2)]. \tag{4.1}$$

We can express mass of the black hole as a function of entropy using the area law $S = \pi r_h^2$, as follows

$$\begin{aligned} M &= \frac{1}{6\sqrt{\pi}} \Big[\left(\pi\beta^2 + S\right)^{3/2} S^{-\frac{3}{2}(\omega+1)} \\ &\quad \left((8PS+3) S^{\frac{3\omega}{2}+\frac{1}{2}} - 3a\pi^{\frac{3\omega}{2}+\frac{1}{2}} \right) \Big]. \end{aligned} \tag{4.2}$$

First law of thermodynamics for this black hole must be modified to include quintessence as follows,

$$dM = TdS + \Psi d\beta + VdP + \mathcal{A}da. \tag{4.3}$$

Where Ψ is the potential conjugate to the magnetic charge β and $\mathcal{A}$ is a quantity

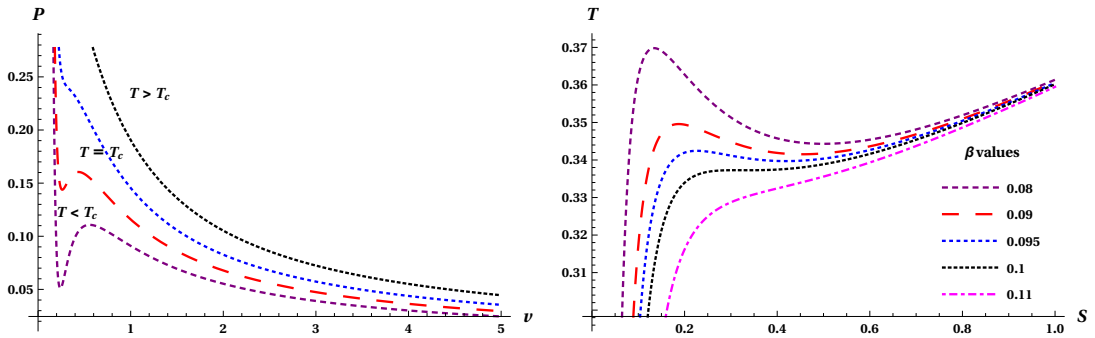

Figure 4.1: To the left we have $P-v$ diagram for regular AdS black hole surrounded by quintessence ($a=0.07$, $\beta=0.1$, $\omega=-2/3$, $T_c=0.36$). In the right side $T-S$ plot for different values of β is shown.

conjugate to quintessence parameter a.

$$\mathcal{A}=\left(\frac{\partial M}{\partial a}\right)_{S,\beta,P}=-\frac{1}{2r_h^{3\omega}}. \tag{4.4}$$

In the extended phase space cosmological constant is considered as thermodynamic pressure.

$$P=-\frac{\Lambda}{8\pi},\ \ \Lambda=-\frac{3}{l^2}. \tag{4.5}$$

We can derive Hawking temperature (equation 4.6) from the first law, which can be combined with the area law to obtain equation of state (equation 4.7).

$$T=\left(\frac{\partial M}{\partial S}\right)_{\Psi,P,a}=\frac{1}{4}\sqrt{\beta^2+\frac{S}{\pi}}S^{-\frac{3\omega}{2}-\frac{5}{2}}\left(3a\pi^{\frac{3\omega}{2}+\frac{1}{2}}\left(\pi\beta^2(\omega+1)+S\omega\right)+S^{\frac{3\omega}{2}+\frac{1}{2}}\left(-2\pi\beta^2+8PS^2+S\right)\right. \tag{4.6}$$

$$P=\frac{1}{8\pi}\left[\frac{8\pi T}{\sqrt{4\beta^2+v^2}}+32\beta^2v^{-3\omega-5}\left(v^{3\omega+1}-3a8^{\omega}(\omega+1)\right)-3a8^{\omega+1}\omega v^{-3(\omega+1)}-\frac{4}{v^2}\right] \tag{4.7}$$

where $v=2r_h$ is specific volume. Using the above equations the $P-v$ and $T-S$ curves are plotted in figure (**??**) and (**??**). These two plots clearly show critical phenomena

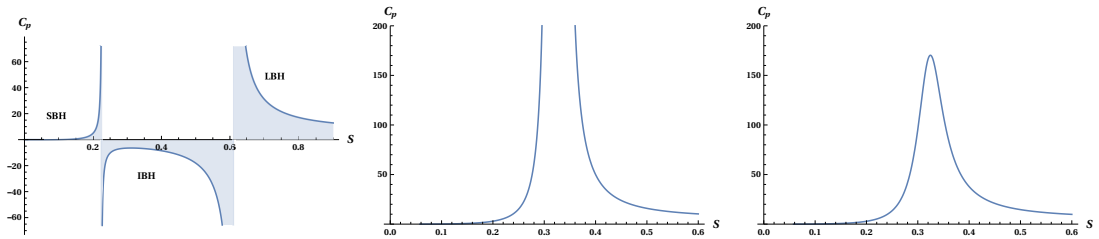

Figure 4.2: Specific heat versus entropy diagram for regular AdS black hole surrounded by quintessence ($a = 0.07$, $\beta = 0.1$, $\omega = -\frac{2}{3}$). (**??**) for $P = Pc$, (**??**) for $P < Pc$, (**??**) for $P > Pc$.

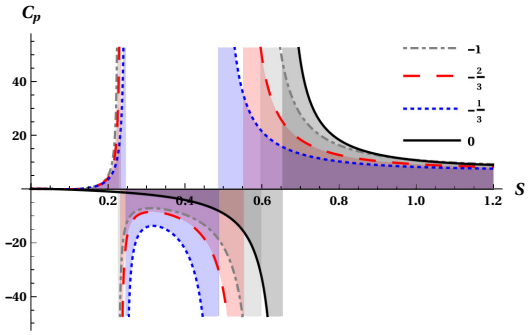

Figure 4.3: Specific heat for different ω values

around the critical points. The critical points are obtained from the conditions,

$$\frac{\partial P}{\partial v} = 0 \quad , \qquad \frac{\partial^2 P}{\partial v^2} = 0. \tag{4.8}$$

In the absence of quientessence, the critical volume (V_c), critical temperature (T_c) and critical pressure (P_c) of regular Bardeen-AdS black hole are obtained, which are as follows,

$$V_c = 2\sqrt{2}\beta\sqrt{2+\sqrt{10}} \quad , T_c = \frac{25\left(13\sqrt{10}+31\right)}{432\pi\beta\left(2\sqrt{10}+5\right)^{3/2}} \quad ,$$

$$P_c = \frac{5\sqrt{10}-13}{432\pi\beta^2}$$

Using the critical quantities, we can calculate $\frac{P_c v_c}{T_c}$ ratio.

$$\frac{P_c v_c}{T_c} = \frac{\left(-26+10\sqrt{10}\right)\left(5+2\sqrt{10}\right)^{3/2}\sqrt{2\left(2+\sqrt{10}\right)}}{775+325\sqrt{10}}$$

which is numericaly equal to 0.381931. For Reissner-Nordström AdS black hole, this ratio matches with that of a Van der Waals gas ($\frac{P_c v_c}{T_c} = 3/8$).

Presence of quientessence affects the phase transition. As the analytic expression is difficult to obtain, the critical quantities are obtained numerically for the state parameter $\omega = -1, -2/3, -1/3$ (table 4.1). Increase in the value of ω from -1 to 0, leads to decrease in the ratio, which approaches to $3/8$.

In statistical mechanics, a phase transition is characterised by divergences in second moments like specific heat, compressibility and susceptibility. Hence to study more details of phase transition we focus on heat capacity of the system. Sign of heat capacity tells about the thermodynamic stability of black hole, which is positive for stable and negative for unstable. The heat capacity at constant pressure is given by,

$$C_P = T\left(\frac{\partial S}{\partial T}\right)_P = \frac{2S\left(\pi\beta^2+S\right)\left(S\left(\sqrt{\pi}(8PS+1)-2a\sqrt{S}\right)+\beta^2\left(\pi a\sqrt{S}-2\pi^{3/2}\right)\right)}{\sqrt{\pi}\left(\beta^4\left(8\pi^2-3\pi^{3/2}a\sqrt{S}\right)+S^2(8PS-1)+4\pi\beta^2 S\right)}$$

$C_P - S$ plot is obtained from this equation, which shows critical behavior (figure 4.2) below certain pressure (P_c) . Figure (4.2) shows that below the critical pressure $P < P_c$, there are two singular points, which reduce to one when $P = P_c$, and above $P > P_c$, these divergence disappears. In figure (**??**), there are three distinct regions seperated by two singular points. The Small black hole (SBH) and large black hole (LBH) regions with positive specific heat, and the intermediate black hole (IBH) with negative specific heat. As the positive specific heat regions are thermodynamicaly stable, phase transition takes place between small black hole and large black hole. From figure(4.3), we observe that the quintesssence state parameter ω shifts the SBH-LBH transition to lower entropy values. The specific heat plotted with $\omega = -1, -\frac{1}{3}, -\frac{2}{3}$ and 0 shows the deviation. When $\omega = 0$, the intermediate region vanishes. Only two regions exists, one with negative and

Table 4.1: Critical points are found using equation (4.8) with quientessence state parameter $\omega = -1, -2/3, -1/3$. The ratio $\frac{P_c v_c}{T_c}$ is calulated for each case.

ω	P_c	v_c	T_c	$\frac{P_c v_c}{T_c}$
-1	0.2155	0.6426	0.3485	0.3973
$-2/3$	0.2073	0.6422	0.3376	0.3945
$-1/3$	0.1926	0.6426	0.3241	0.3819

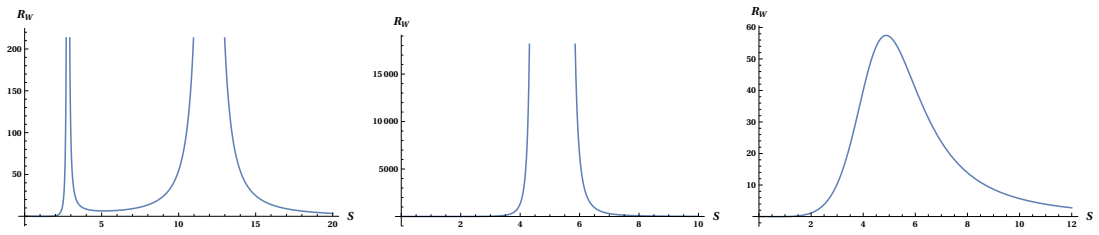

Figure 4.4: Curvature divergence plots for Weinhold metric. In all three plots quintessence parameter and monopole charge are fixed, $a = 0.5$ and $\beta = 1$. Pressure is $P = 0.01$ in (**??**), $P = 0.01264$ in (**??**) and $P = 0.0141$ in (**??**).

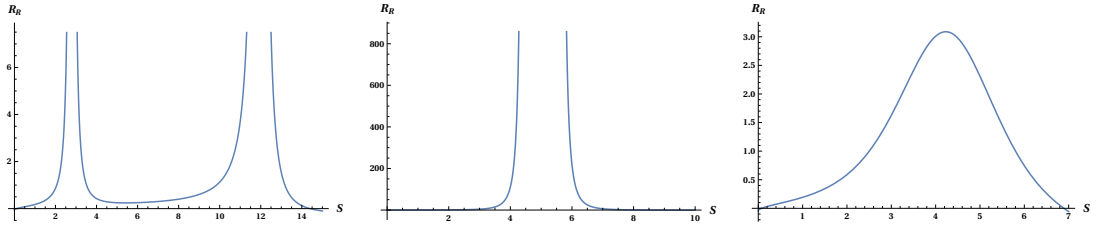

Figure 4.5: Curvature divergence plots for Ruppeiner metric. In all three plots quintessence parameter and monopole charge are fixed, $a = 0.5$ and $\beta = 1$. Pressure is $P = 0.01$ in (**??**), $P = 0.01264$ in (**??**) and $P = 0.0141$ in (**??**).

other with positive specific heat, the behavior is similar to that of regular Bardeen black hole (**?**).

The small–large black hole phase transition observed in this black hole is analogous to the liquid–gas transition in Van der Waals gas like in Reissner-Nordström AdS black holes. The notable difference compared to Van der Waals gas is the ratio $\frac{P_c v_c}{T_c}$, which doesnot appear to be a constant value 3/8, as the critical temperature T_c depends on the quintessence.

4.3 Thermodynamic Geometry

In this section we investigate thermodynamic phase transtions based on geometric formalism proposed by Weinhold, Ruppeiner and Quevado. The thermodynamic geometry is a possible tool to explore thermodynamic phase transitions from microscopic point of view. The thermodynamic scalar curvature R is directly proportional to the correlation volume of the system $R \propto \xi^d$, where d is spatial dimensionality. The divergent behavior of curvature scalar ploted against entropy reflects the existance of critical points corresponding to thermodynamic phase transition.

4.3.1 Weinhold Geometry

The Weinhold metric is defined adhoc in the thermodynamic equilibrium space as the Hessian of the internal energy M,

$$ds^2_W = g^W_{ij} dx^i dx^j = \partial_i \partial_j M(S, N^a) dx^i dx^j \quad , \quad (i, j = 1, 2)$$

where N^a represents any other thermodynamic extensive variables. Here, mass M is the function of entropy S and extensive variable β, which is the monopole charge. A Hessian is defined as a square matrix containing second derivative of energy with respect to the entropy and other extensive parameters(**??**),

$$g^W = \begin{bmatrix} M_{,SS} & M_{,S\beta} \\ M_{,\beta S} & M_{,\beta\beta} \end{bmatrix}.$$

Using the expression for mass of the black hole (equation 4.2), the components of metric tensor turns out to be,

$$g_{SS} = \frac{\beta^4 \left(8\pi^2 - 3\pi^{3/2} a\sqrt{S}\right) + S^2(8PS - 1) + 4\pi\beta^2 S}{8\sqrt{\pi} S^3 \sqrt{\pi\beta^2 + S}} \tag{4.9}$$

$$g_{S\beta} = g_{\beta S} = \frac{\beta\left(\beta^2\left(3\sqrt{\pi} a\sqrt{S} - 6\pi\right) + S(8PS - 3)\right)}{4S^2\sqrt{\beta^2 + \frac{S}{\pi}}} \tag{4.10}$$

$$g_{\beta\beta} = \frac{\left(2\pi\beta^2 + S\right)\left(\sqrt{\pi}(8PS + 3) - 3a\sqrt{S}\right)}{2S\sqrt{\pi\beta^2 + S}}. \tag{4.11}$$

From metric tensor g^W_{ij}, one can calculate curvature scalar, which is found to be a complicated expression, $R_W(S, P, b, \omega, a)$. Ploting the curvature R_W versus entropy S, we have studied its divergence behavior, which occur at mulitiple points (figure 4.4). Even at the critical point (P_c=0.207 for a=0.07 and $\beta = 0.1$), R_W shows multiple divergences (figure **??**) which are different from that of the critical value of entropy (S) observed in specific heat plots. From these randomly located diverging points we can infer only the critical behavior of the system, but not the exact phase transition points.

As there is no agreement between the divergence points in Weinhold geometry and specific heat study, next we focus on Ruppeiner geometry.

4.3.2 Ruppeiner Geometry

The Ruppeiner metric is defined as a Hessian of the entropy function S of the system instead of the internal energy M as in the Weinhold case. But one can transform Ruppeiner metric, which is a function of M and β originally, to the same coordinate system used in Weinhold metric i.e., S and β. Technically, their geometries are related to each other conformally (**????**).

The Ruppeiner metric in the thermodynamic space states is given as ,

$$g^R_{ij} = -\partial_i \partial_j S(M, x^\alpha) \qquad (i, j = 1, 2)$$

$$g^R = \begin{bmatrix} S_{,MM} & S_{,M\beta} \\ S_{,\beta M} & S_{,\beta\beta} \end{bmatrix}.$$

Because of the conformal property, the line elements in Ruppeiner and Weinhold formalism are related as

$$dS^2_R = -\frac{dS^2_W}{T}. \tag{4.12}$$

Using (4.9), (4.10), (4.11) and (4.6) the components of Ruppeiner metric tensor are easily obtained as ,

$$g_{SS} = \frac{\sqrt{\pi}\left(b^4\left(8\pi^2 - 3\pi^{3/2}a\sqrt{S}\right) + 4\pi b^2 S + S^2(8PS-1)\right)}{2S(\pi b^2+S)\left(b^2\left(\pi a\sqrt{S} - 2\pi^{3/2}\right) + S\left(\sqrt{\pi}(8PS+1) - 2a\sqrt{S}\right)\right)} \tag{4.13}$$

$$g_{S\beta} = g_{\beta S} = \frac{\pi^{3/2} b\left(b^2\left(6\pi - 3\sqrt{\pi}a\sqrt{S}\right) + S(3-8PS)\right)}{(\pi b^2+S)\left(b^2\left(2\pi^{3/2} - \pi a\sqrt{S}\right) - S\left(\sqrt{\pi}(8PS+1) - 2a\sqrt{S}\right)\right)} \tag{4.14}$$

$$g_{\beta\beta} = \frac{2\pi S\left(2\pi b^2+S\right)\left(\sqrt{\pi}(8PS+3) - 3a\sqrt{S}\right)}{(\pi b^2+S)\left(b^2\left(\pi a\sqrt{S} - 2\pi^{3/2}\right) + S\left(\sqrt{\pi}(8PS+1) - 2a\sqrt{S}\right)\right)}. \tag{4.15}$$

The curvature tensor R_R calculated from the above metric g^R_{ij} is again a complicated

expression like in Weinhold case. The obtained curvature function is plotted against entropy S to study the critical behavior (figure 4.5 and **??**).

The figure (**??**) shows that at the critical point $P_c = 0.207$, there are multiple divergence around $S = 0.06$ and $S = 0.48$, which does not correspond to the critical value of entropy $(S = 0.32)$. From these multiple singularities for curvature scalar, it is difficult to identify the critical points from Ruppeiner geometry. But it is interesting that Ruppeiner geometry indicates a phase transition even though it cannot identify the exact transition points (4.5), like Weinhold geometry. This kind of anomalies were found in Kehagias-Sfetsos black hole **?** and in Gauss-Bonnet Born-Infeld massive gravity theories **??**. In both Weinhold and Ruppeiner geometries we note that, the number of divergence points reduces of curvature scalar decreases when the pressure increases and gradually dissapear.

4.3.3 Geometrothermodynamics

In this approach, the metric is constructed from a Legendre invariant thermodynamic potential and their derivatives with respect to the extensive variables. For geometrothermodynamic calculations, we will consider $2n+1$ dimensional thermodynamic phase space $\mathcal{T}$. This phase space is constructed using the cordinates $\{\Phi, E^a, I^a\}$, where Φ is thermodynamic potential and E^a and I^a are extensive and intensive variables. Then Gibbs one-form is introduced as $\Theta = d\Phi - \delta_{ab} I^a E^b$, satisfying $\Theta \wedge (d\Theta) \neq 0$. Defining a Legendre invariant metric G on $\mathcal{T}$,

$$G = (d\Phi - \delta_{ab} I^a E^b)^2 + (\delta_{ab} I^a E^b)(\eta_{cd} I^c E^d) \tag{4.16}$$

$$\eta_{cd} = diag(-1, 1, ...1). \tag{4.17}$$

$\mathcal{T}$, Θ and G constitutes a Riemann contact manifold. Following this we define an n dimensional Riemannian submanifold $\varepsilon \subset \mathcal{T}$, which is the space of equilibrium thermodynamic states (equilibrium manifold) via a smooth map $\varphi : \varepsilon \to \mathcal{T}$. The Quevedo metric, which is similar to Ruppeiner and Weinhold metric, is defined on this equilibrium submanifold using the inverse map $\varphi^*(G)$.

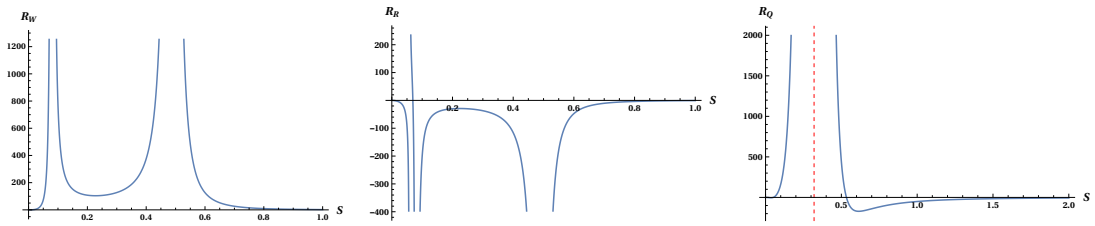

Figure 4.6: Curvature divergence plots for Weinhold (**??**), Ruppeiner (**??**) and Quevado metric (**??**) around critical point ($a = 0.5, \beta = 0.1$ and $P_c = 0.207$).

$$g^Q = \varphi^*(G) = \left(E^c \frac{\partial \Phi}{\partial E^c}\right)\left(\eta_{ab}\delta^{bc}\frac{\partial^2 \Phi}{\partial E^c \partial E^d} dE^a dE^d\right) \tag{4.18}$$

In our case we consider a 5 dimensional phase space with the coordinates $Z_A = \{M, S, \beta, T, \Theta\}$, where S, β are extensive variables and T, Θ are their dual intensive variables. Then we have the fundamental Gibbs one form as,

$$\Theta = dM - TdS - \Psi d\beta. \tag{4.19}$$

Now we can write the Quevedo metric as follows,

$$g^Q = \left(SM_S + \beta M_\beta\right)\begin{bmatrix} -M_{SS} & 0 \\ 0 & M_{\beta\beta} \end{bmatrix}. \tag{4.20}$$

Using the Quevedo metric we calculate the corresponding curvature, which is a complicated expression having the following form,

$$R_Q = \frac{f(S, \beta, P, a)}{g(S, \beta, P, a)}, \tag{4.21}$$

which is intersting as it has a diverging behavior. Using the plots of curvature scalar R_Q, we investigate the divergence. In the figure(**??**), we can see a divergence peaked at $S \approx 0.32$ same as in the specific heat case. Contrary to what we obtained in Weinhold and Ruppeiner geometries, the singular point of curvature scalar in geometrothermodynamics exactly matches the specific heat singular point.

4.4 Conclusion

We have studied the thermodynamics and thermodynamic geometry of a regular Bardeen-AdS black hole surrounded by a quintessence. In the thermodynmic study we observed a critical behavior from $P-v$ and $T-S$ plots. Further confirmation was obtained from the specific heat plots. The discontinuity in the specific heat at $S = 0.32$ indicates a phase transition of the system. We analysed the effect of quientessence in the phase transitions through the state parameter ω. The critical values for pressure (P_c), volume (v_c) and temperature (T_c) are obtained for $\omega = -1, -\frac{2}{3}$ and $-\frac{1}{3}$ case. The ratio $\frac{P_c v_c}{T_c}$ showed slight decrease with increase of ω from -1 to $-\frac{1}{3}$.

Following the study of black hole phase transition in the thermodynamic approach we carried out the geometrical investigation of the same. In the literature it is a well known fact that the divergence behavior of curvature scalar also reflects the existance of critical points. If we accept that the criticality of specific heat as the definition of phase transition, the thermodynamic geometry which shows divergence at the same point turns out be the correct geometrical description of the same phenom ena. For the metric under consideration we found that, eventhough the Ruppeiner and Weinhold geometries reflect singularity of curvature scalar, it can only be taken as the indication of phase transition but not the accurate description of the same, as the diverging points do not coincide with that of specific heat. There were multiple divergence and mismatch in the thermodynamic scalar of Weinhod and Ruppeiner geometries. This indicates an anomaly, to overcome this we have used Quevado's geometrothermodynamics. Main problem with the Weinhold and Ruppeiner geometry is that, they were not Legendre invariant and thus depends on the choice of thermodynamic potential. However, geometrothermodynamics being Legendre invariant reproduces critical point exactly.

As a future work, we would like to apply thermodynamic approach formulated by S. Hendi *et al.* **?**.But the discripancy among the different geometrical discription in validating the critical behavior is still not clear conceptually, the solution to this may lie in the domain of quantum gravity.

Chapter 5

Classical thermodynamics and Holography

Chapter 6

Summary and Future Work

Appendices

Appendix A

Appendix B

Bibliography

Bardeen, J. M., Carter, B., and Hawking, S. W. (1973). The Four Laws of Black Hole Mechanics. *Commun. math. Phys*, 31:161–170.

Barriola, M. and Vilenkin, A. (1989). Gravitational field of a global monopole. *Phys. Rev. Lett.*, 63:341–343.

Bekenstein, J. (1972). Black holes and the second law. *Lettere Al Nuovo Cimento (1971–1985)*, 4:5–8.

Bekenstein, J. D. (1973). Black holes and entropy. *Physical Review D*, 7(8):2333–2346.

Bekenstein, J. D. (1974). Generalized second law of thermodynamics in black-hole physics. *Physical Review D*, 9(12):3292–3300.

Chamblin, A., Emparan, R., Johnson, C. V., and Myers, R. C. (1999a). Charged AdS black holes and catastrophic holography. *Physical Review D - Particles, Fields, Gravitation and Cosmology*, 60(6):1–17.

Chamblin, A., Emparan, R., Johnson, C. V., and Myers, R. C. (1999b). Holography, thermodynamics and fluctuations of charged AdS black holes. *Phys. Rev.*, D60:104026.

Chen, S., Wang, L., Ding, C., and Jing, J. (2010a). Holographic superconductors in the AdS black hole spacetime with a global monopole. *Nucl. Phys.*, B836:222–231.

Chen, S., Wang, L., Ding, C., and Jing, J. (2010b). Holographic superconductors in the AdS black-hole spacetime with a global monopole. *Nuclear Physics B*, 836:222–231.

Davies, W. (1978). Thermodynamics of black holes. *Rep. Prog. Phys*, 41.

Deng, G.-M., Fan, J., Li, X., and Huang, Y.-C. (2018). Thermodynamics and phase transition of charged AdS black holes with a global monopole. *International Journal of Modern Physics A*, 33(03):1850022.

Dolan, B. P. (2011). Pressure and volume in the first law of black hole thermodynamics. *Class. Quantum Grav*, 28:235017–13.

Ghaffarnejad, H., Yaraie, E., and Farsam, M. (2018). Quintessence Reissner Nordström Anti de Sitter Black Holes and Joule Thomson effect. *Int. J. Theor. Phys.*, 57(6):1671–1682.

Gunasekaran, S., Mann, R. B., and Kubiznak, D. (2012). Extended phase space thermodynamics for charged and rotating black holes and Born-Infeld vacuum polarization. *JHEP*, 11:110.

Hawking, S. W. and Page, D. N. (1983). Communications in Mathematical Physics Thermodynamics of Black Holes in Anti-de Sitter Space. *Commun. Math. Phys*, 87:577–588.

Jacobson, T. (1996). Introductory lectures on black hole thermodynamics. *Given at Utrecht U. in*, pages 30–59.

Johnson, C. V. (2014). Holographic heat engines. *Classical and Quantum Gravity*, 31(20):205002.

Johnston, D. C. (2014). Thermodynamic Properties of the van der Waals Fluid.

Kibble, T. W. B. (1976). Topology of cosmic domains and strings. *J. Phys. A: Math. Gen*, 9(8).

Kubizňák, D. and Mann, R. B. (2012). P - V criticality of charged AdS black holes. *Journal of High Energy Physics*, 2012(7).

Kubizňák, D., Mann, R. B., and Teo, M. (2017). Black hole chemistry: thermodynamics with lambda. *Classical and Quantum Gravity*, 34(6):063001.

Lan, S.-Q. (2018). Joule-Thomson expansion of charged Gauss-Bonnet black holes in AdS space. arXiv:1805.05817v1.

Landau, L. D. L. D., Lifshit[U+FE20]s[U+FE21], E. M. E. M., Pitaevskiĭ, L. P. L. P., Sykes, J. B., and Kearsley, M. J. (1980). *Statistical physics. Part 1*. Elsevier Butterworth Heinemann.

Maldacena, J. (1999). The Large-N Limit of Superconformal Field Theories and Supergravity. *International Journal of Theoretical Physics*, 38(4).

Mo, J.-X. and Li, G.-Q. (2018). Effects of Lovelock gravity on the Joule-Thomson expansion. arXiv:1805.04327v1.

Mo, J.-X., Li, G.-Q., Lan, S.-Q., and Xu, X.-B. (2018). Joule-Thomson expansion of d-dimensional charged AdS black holes. arXiv:1804.02650v1.

Ökcü, Ö. and Aydıner, E. (2017). Joule–Thomson expansion of the charged AdS black holes. *Eur. Phys. J. C*, 77.

Ökcü, Ö. and Aydıner, E. (2018). Joule–Thomson expansion of Kerr–AdS black holes. *The European Physical Journal C*, 78.

Page, D. N. (2005). Hawking radiation and black hole thermodynamics. *New Journal of Physics*, 7(1):203.

Sahay, A., Sarkar, T., and Sengupta, G. (2010). On the thermodynamic geometry and critical phenomena of AdS black holes. *Journal of High Energy Physics*, 2010(7).

Vilenkin, A. (1985). Cosmic strings and domain walls. *Physics Reports*, 121(5):263–315.

Vilenkin, A. A. and Shellard, E. P. S. E. P. S. (1994). *Cosmic strings and other topological defects*. Cambridge University Press.

Wald, R. M. (2001). The thermodynamics of black holes. *Living Reviews in Relativity*, 4(1):6.

Zemansky, M. W., Dittman, R., and Chattopadhyay, A. K. (2011). *Heat and thermodynamics*. Tata McGraw Hill Education Private Limited.

LIST OF PUBLICATIONS

1. Peer Reviewed International Journals:

1.

2. Peer Reviewed International Journal proceedings:

3. International Conferences Presentations:

CURRICULUM VITAE